**Biophysical Journal, Volume *122***

## Supplemental information

# Role of K364 next to the active site cysteine in voltage-dependent phosphatase activity of Ci-VSP

**Ian Costa Paixao, Natsuki Mizutani, Makoto Matsuda, Rizki Tsari Andriani, Takafumi Kawai, Atsushi Nakagawa, Yoshifumi Okochi, and Yasushi Okamura**

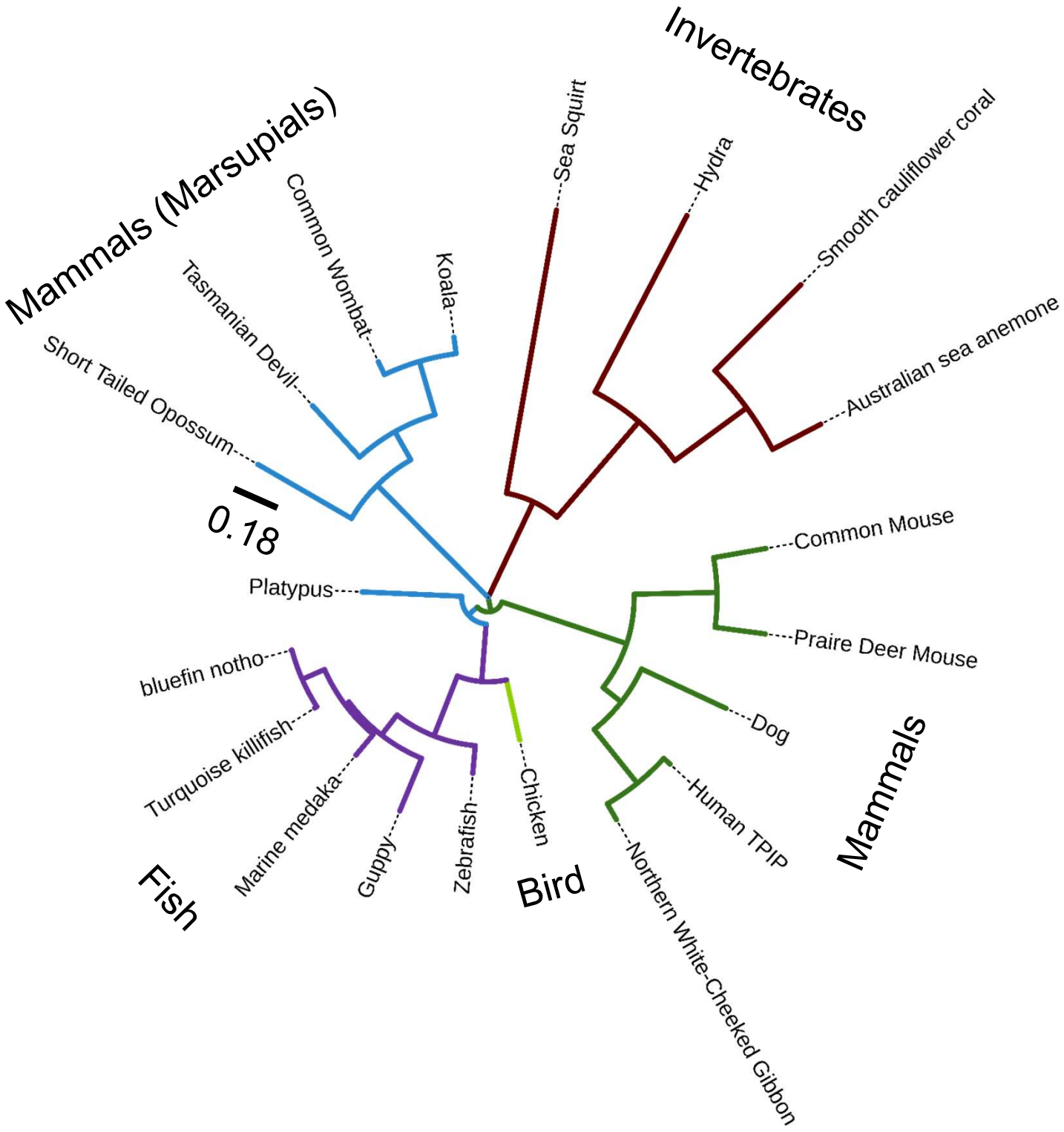


**Figure S1. Phylogenetic tree of mammalian VSP orthologs.**

Phylogenetic tree of VSP orthologs constructed by maximum likelihood test with MEGA 11. Tree is divided in marsupials/mammals in blue, other mammals in green, invertebrates in brown, birds in light green, and fish in purple. Black bar with value is distance scale.

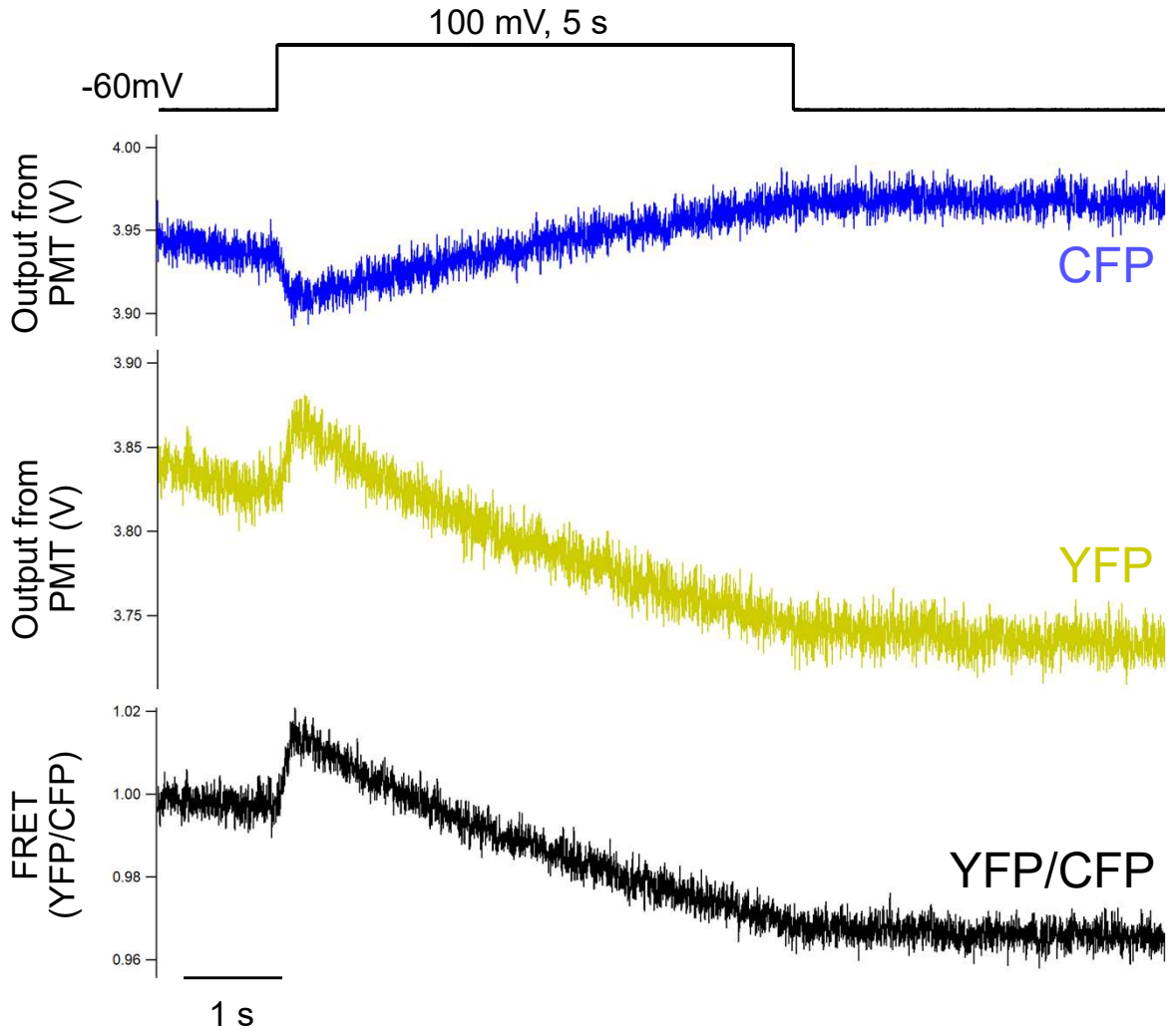


**Figure S2. Raw trace of CFP, YFP, and YFP/CFP ratio signals of F-TAPP probe.**

Representative fluorescence traces of CFP, YFP, and YFP/CFP ratio of F-TAPP recorded from an oocyte expressing WT Ci-VSP upon a depolarizing step to 100 mV for 5 s. Y axis indicates volt of PMT output (CFP and YFP) and ratio (YFP/CFP).

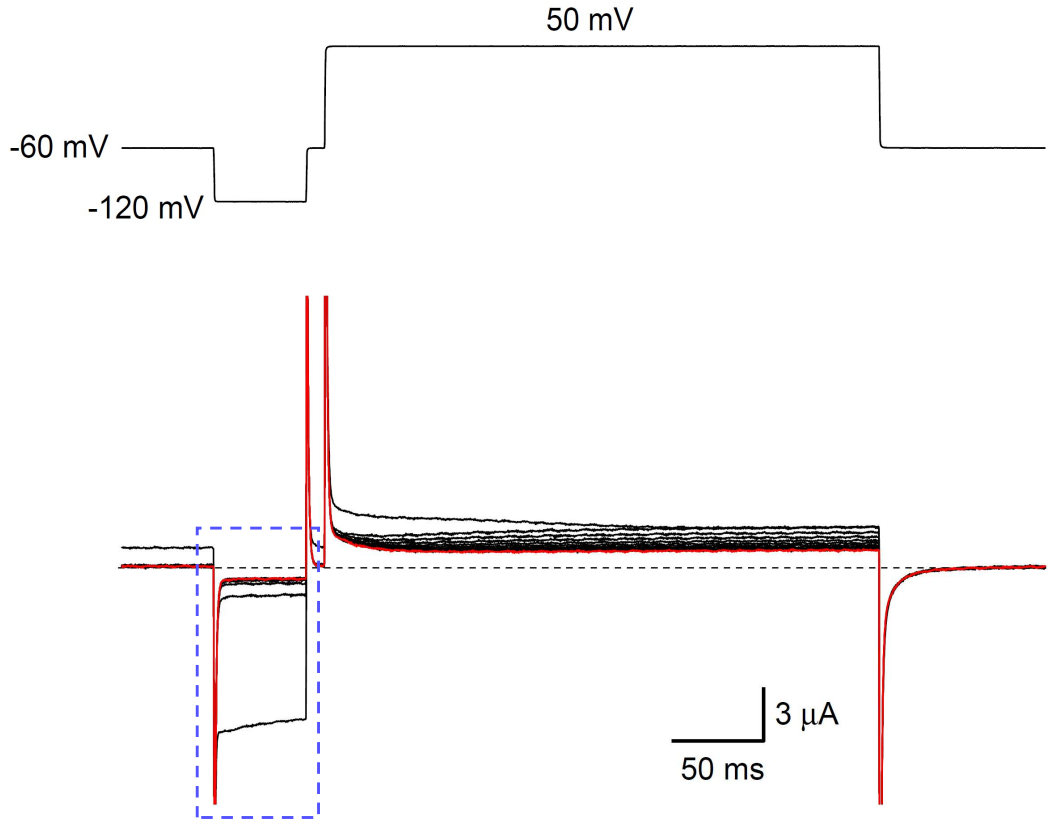


**Figure S3. Protocol to record GIRK2 current.**

Representative GIRK2 current traces in an oocyte expressing WT Ci-VSP (*Bottom*). The pulse protocol (*Top*) composed of a 50-ms test step to -120 mV and 300 ms depolarization (50 mV) was repeated 12 times, and all traces are superimposed. The 12th trace is shown in red. Black dotted line indicates zero current level. Currents recorded during the test pulse (surrounded by a blue dotted square) are shown in Figs. 2*F*, 5*A*, and S4*B*.

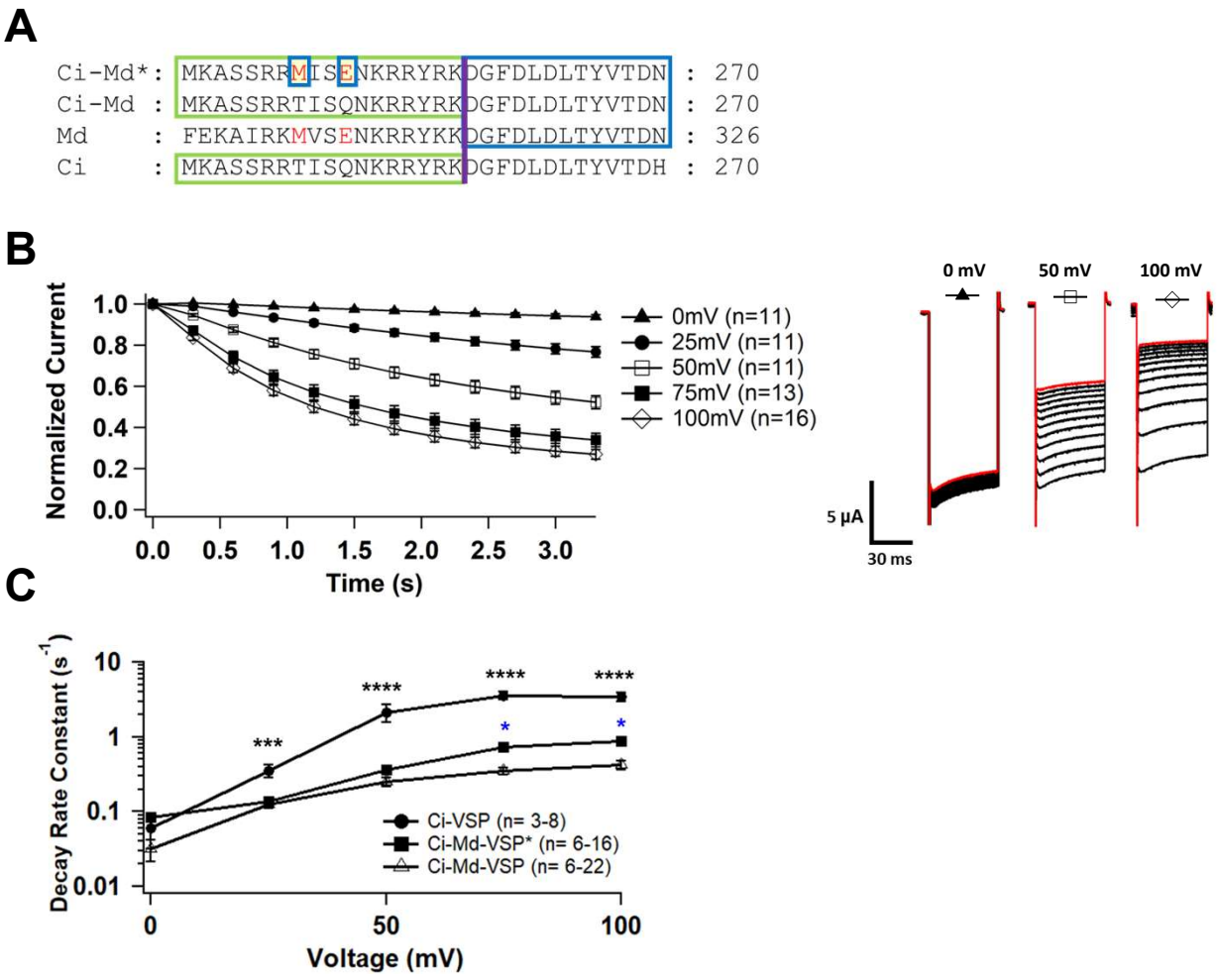


**Figure S4. Characterization of voltage-dependent phosphoinositide phosphatase activity of the *sea squirt-opossum* VSP chimera, Ci-Md-VSP* with the additional mutation of T247M/Q250E in *Xenopus* oocyte.**

(*A*) Amino acid sequences around the junction region of chimeric construction between Ci-VSP; Ci-Md-VSP; and Ci-Md-VSP*. Double mutation of T247M/ Q250E is highlighted in blue. (*B*) Decline time course of Kir current upon voltage-evoked Ci-Md-VSP* activities with five levels of conditioning depolarization (*left*) and the representative raw traces upon -120 mV step with conditioning depolarization to 0 mV, 50 mV and 100 mV (*right*). Data are presented as mean ± standard error (SE). (*C*) Decay rate constant of normalized GIRK2 current at different potentials. GIRK2 was co-expressed with Ci-VSP; Ci-Md-VSP; or Ci-Md-VSP*. * p< 0.05, *** p< 0.001, **** p< 0.0001, one way ANOVA with Tukey's multiple comparisons test. Data are presented as mean ± standard error (SE).

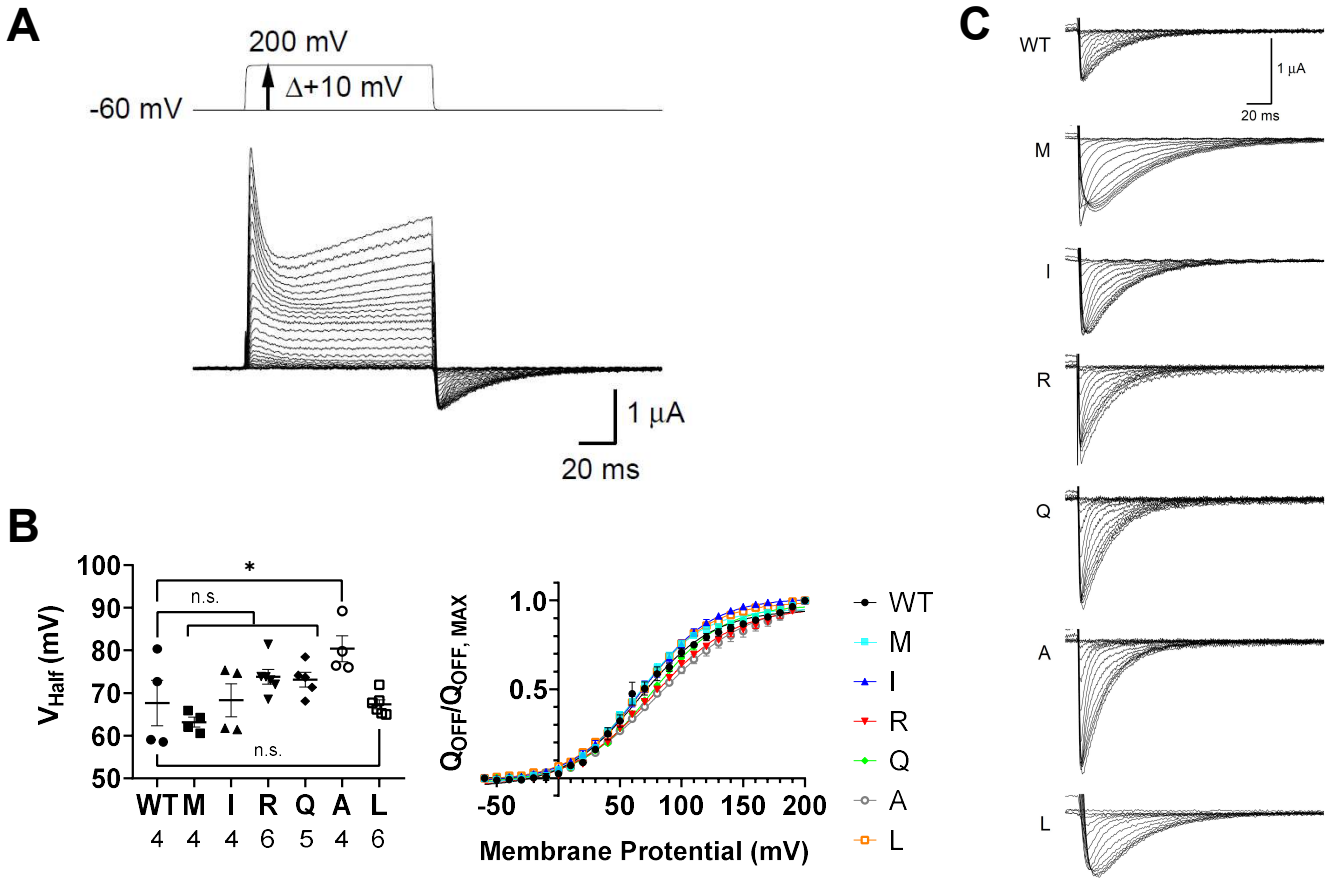


**Figure S5. Sensing current recording suggests similar levels of surface expression and small voltage shift between mutants.**

(*A*) Representative sensing current traces of WT Ci-VSP evoked by depolarizing steps (top). (*B*) $V_{Half}$ (*left*) and $Q_{OFF}$-*V* curve (*right*) of each mutant and Ci-VSP WT. The sensing currents were measured from cells expressing VSP alone and were evoked by depolarizing steps from the holding potential of -60 mV to 200 mV in 10-mV increments. Leak subtraction was performed using a P/-4 protocol. The maximum charges of Off-sensing current ($Q_{OFF}$) was calculated by integration of the off-sensing current which extends 150 ms from the end of depolarizing step. $Q_{OFF}$ was normalized by the maximum charge ($Q_{MAX}$) and plotted against pulse voltage. $Q_{OFF}$-V curves were fitted with the Boltzmann equation: $Q_{OFF}(V)/Q_{MAX} = 1/[1 + exp(-ZF(V-V_{Half})/RT)]$, where *F* is Faraday constant, *R* is the gas constant, *T* is the absolute temperature, *Z* is the effective valency, V is voltage, and $V_{Half}$ is the voltage that gives half of the maximum $Q_{OFF}$ ($Q_{MAX}$). Data are presented as mean ± standard error (SE). * $p<0.05$, n.s.; statistically not significant, one way ANOVA followed by Dunnett's test. (*C*) Representative off-sensing current traces measured by the protocol shown in (*A*). Traces are shown every 20-mV increment.

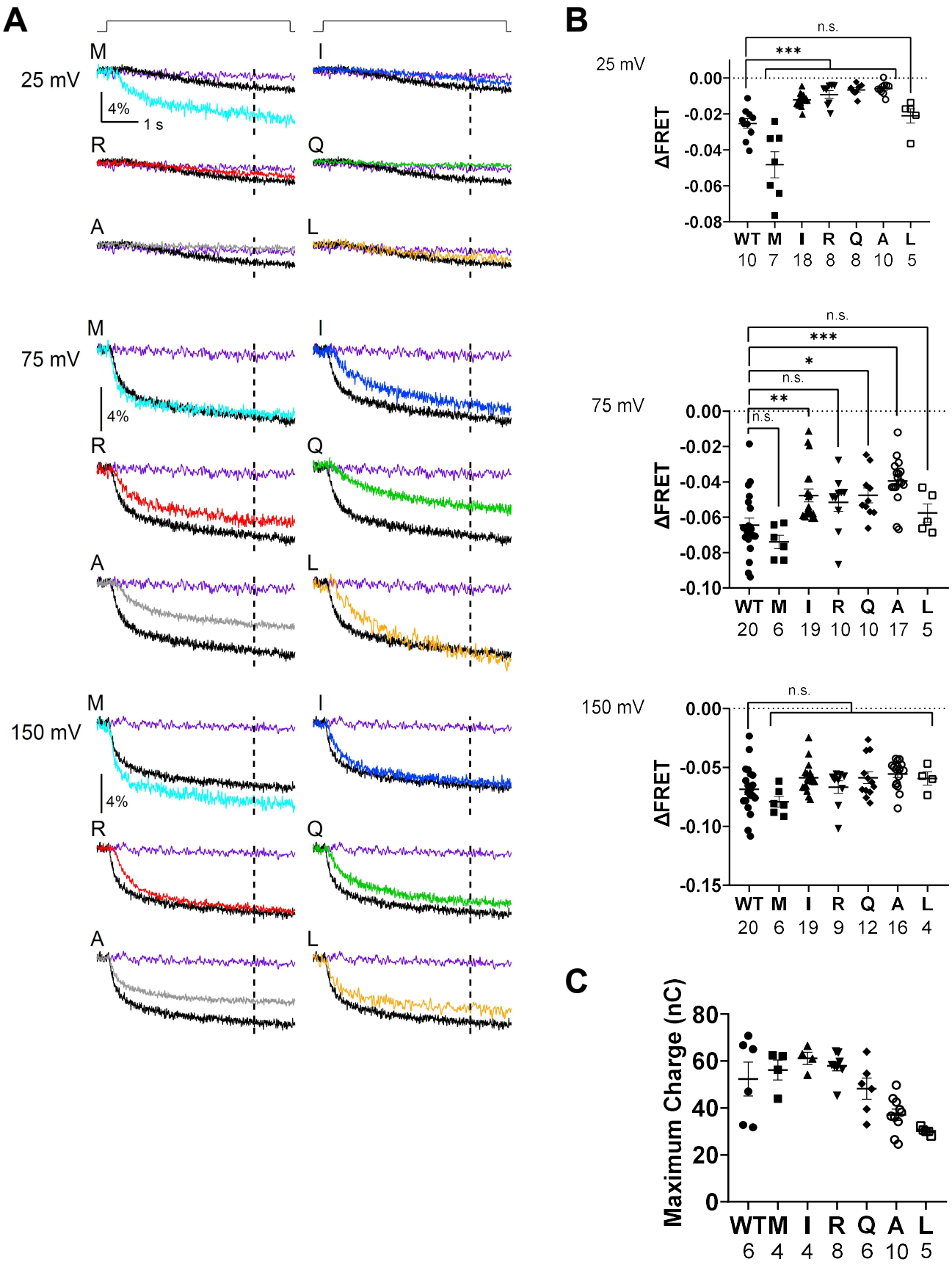


**Figure S6. Voltage-dependent change of FRET signal of PI(4,5)$P_2$-sensing probe, F-PLC, coexpressed with K364 mutant Ci-VSPs in *Xenopus* oocyte.**

(*A*) Representative traces of F-PLC YFP/CFP ratio signal measured at 25 mV (*Top*), 75 mV (*Middle*), and 150 mV (*Bottom*); Depolarizing step shown in top of traces was applied from a holding potential of -60 mV to indicated value for 5 seconds. Dotted line in each trace indicates the time point (at 4 s after the beginning of depolarization) for calculating ΔFRET. (*B*) FRET signal change from the resting level measured at 4 s after initiation of voltage step. Each trace from 0 to 150 mV was obtained from the same oocytes. Data are from the same set as in Fig.4 (0, 50, 100 mV) and complementary to each other. Data are presented as mean ± standard error (SE). * p<0.05, ** p<0.01, *** p<0.001, n.s.; statistically not significant, one way ANOVA followed by Dunnett's test. (*C*) Maximum moving charges calculated from Off-sensing currents at 160 mV, representing cell surface expression level. Data are presented as mean ± standard error (SE).

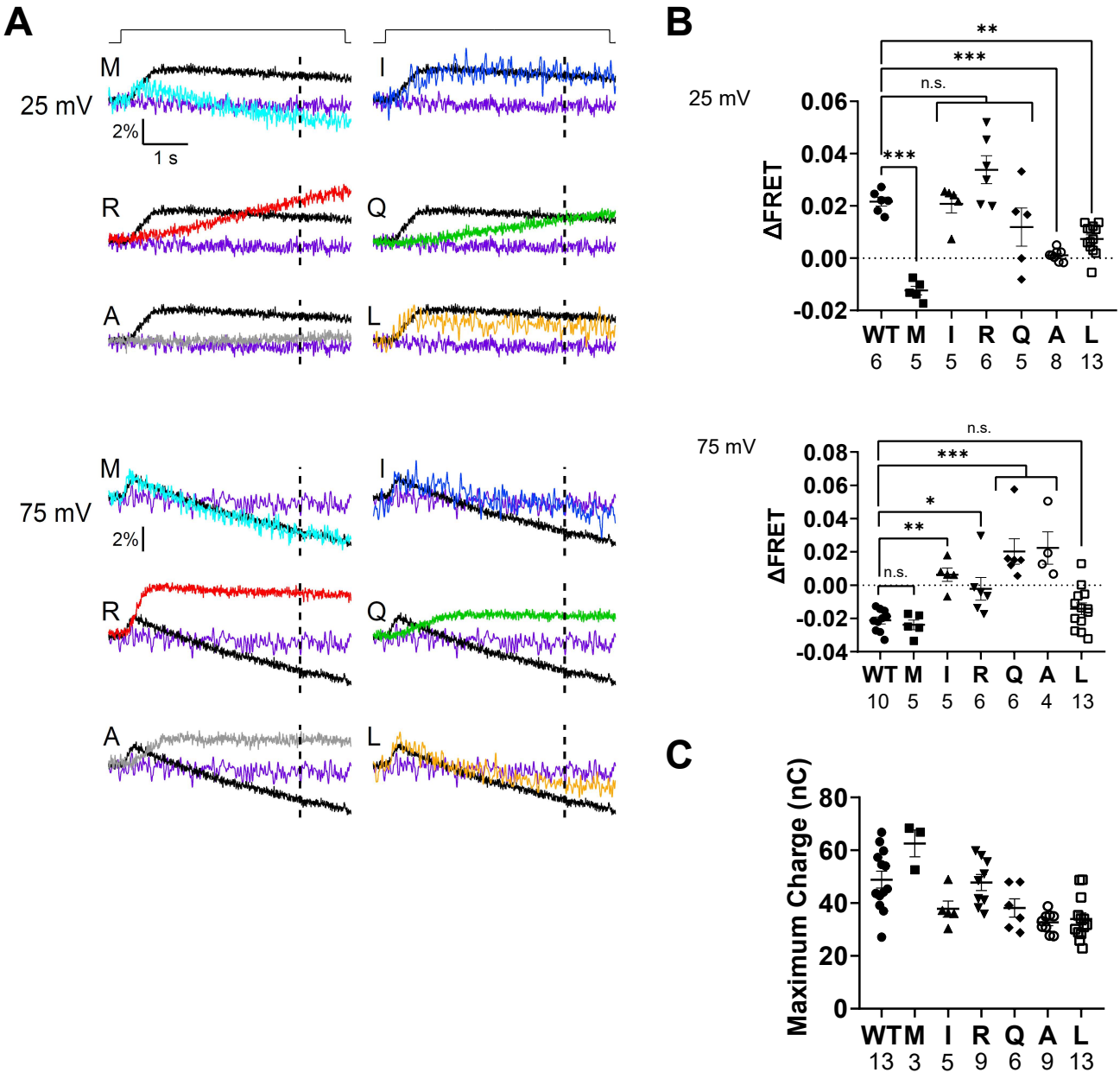


**Figure S7. Voltage-dependent change of FRET signal of PI(3,4)$P_2$-sensing probe, F-TAPP, coexpressed with K364 mutant Ci-VSPs in *Xenopus* oocyte.**

(*A*) Representative traces of F-TAPP YFP/CFP ratio signal measured at 25 mV (*Top*) and 75 mV (*Bottom*); Depolarizing step shown in top of traces was applied from a holding potential of -60 mV to indicated value for 5 seconds. Dotted line in each trace indicates the time point (at 4 s after the beginning of depolarization) for calculating ΔFRET. (*B*) FRET signal change from the resting level measured at 4 s after initiation of voltage step. Each trace from 0 to 150 mV was obtained from the same oocytes. Data are from the same set as in Fig.6 (0, 50, 100, 150 mV) and complementary to each other. Data are presented as mean ± standard error (SE). * $p<0.05$, ** $p<0.01$, *** $p<0.001$, n.s.; statistically not significant, one way ANOVA followed by Dunnett's test. (C) Maximum moving charge calculated from Off-sensing currents at 160 mV, representing cell surface expression level. Data are presented as mean ± standard error (SE).

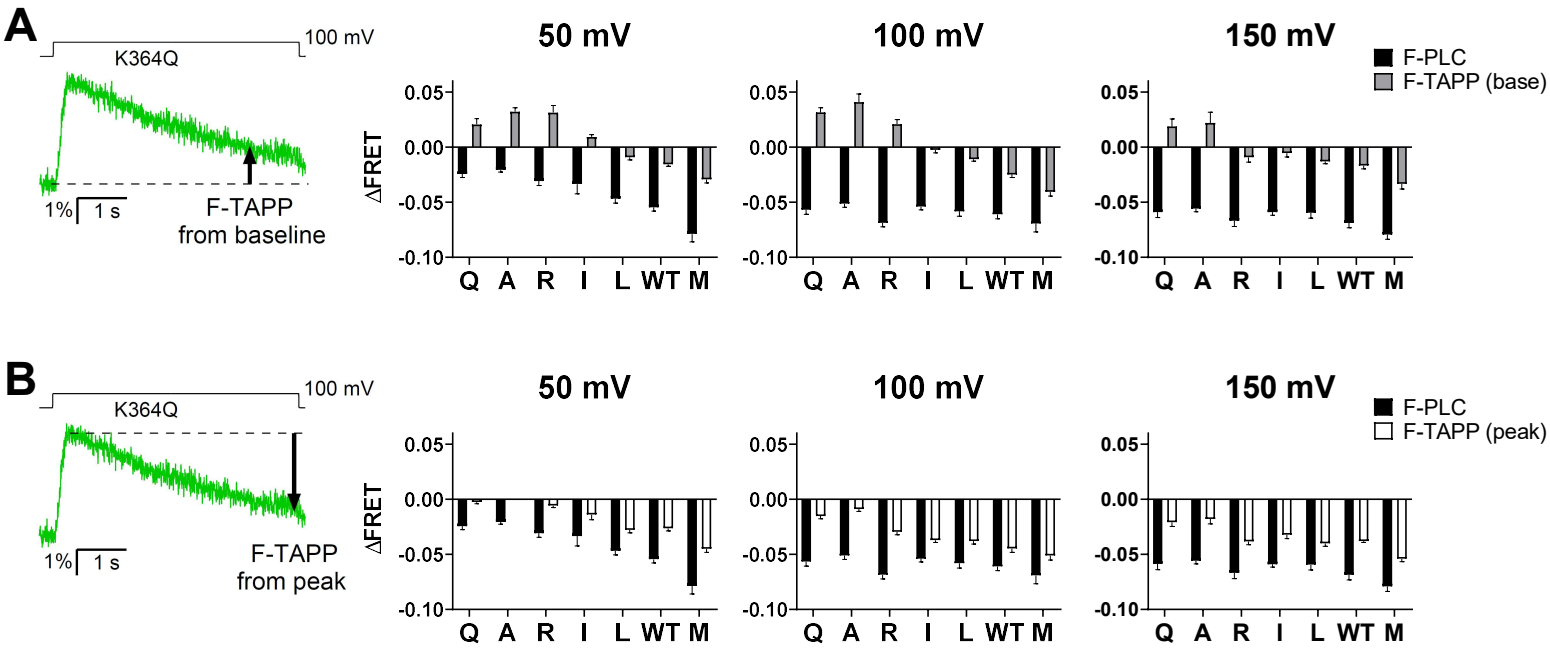


**Figure S8. Summary of $PI(3,4)P_2$ versus $PI(4,5)P_2$ phosphatase activity of Ci-VSP K364 mutants and wild type.**

Graph showing voltage dependent signals of F-TAPP FRET from the baseline for (A) or from the peak for (B) with F-PLC FRET representing $PI(4,5)P_2$ phosphatase activity (subreaction from $PI(4,5)P_2$ to PI(4)P (Fig. 2*A*)). Data for F-PLC FRET in B is the same as in A. Data for membrane depolarization to 50, 100 and 150 mV are presented as mean ± standard error (SE). Sample size is described in Fig. 4*B* and S6*B* for F-PLC, and in Fig. 6*B* for F-TAPP.

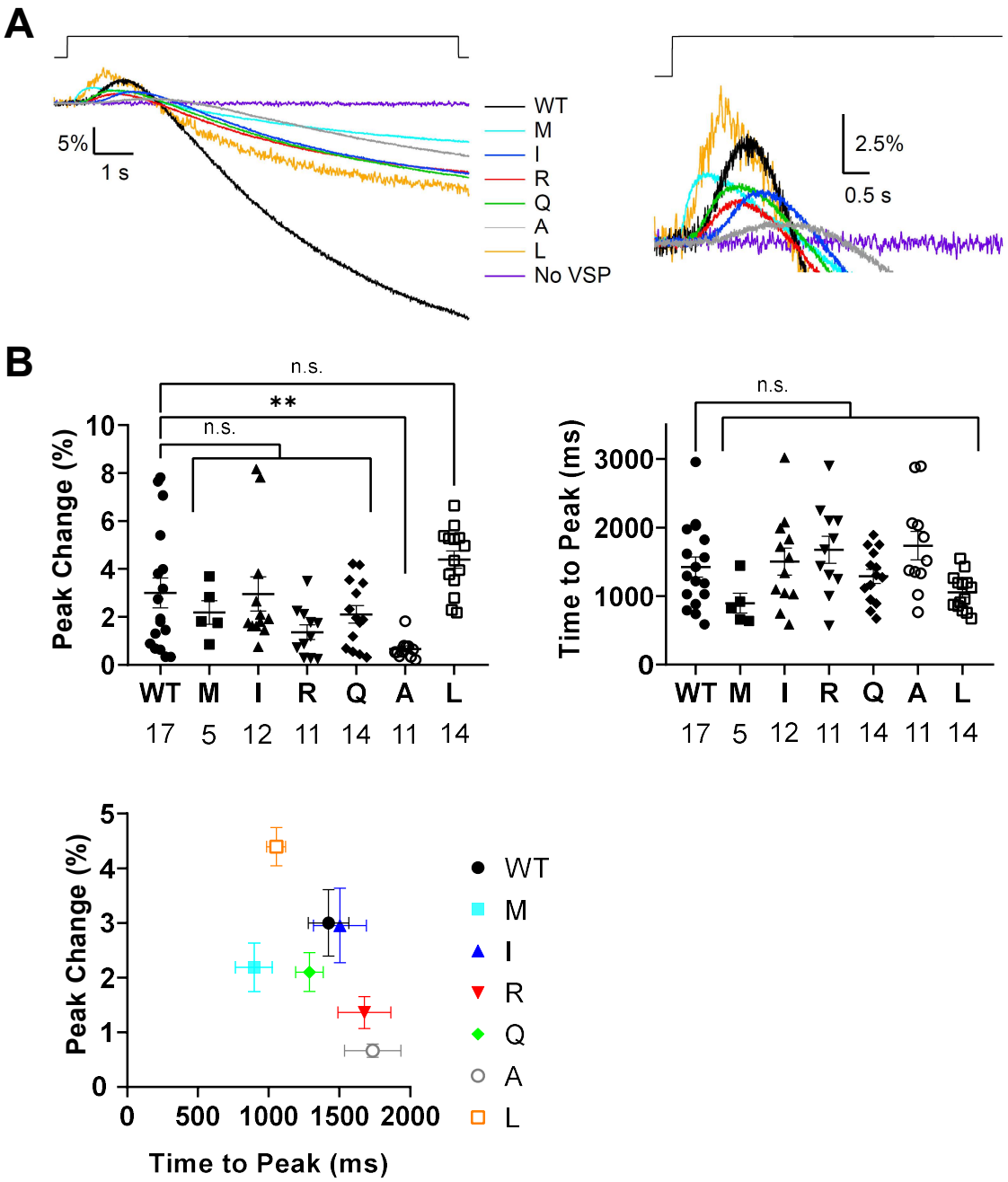


**Figure S9. Comparison of subreaction of 3-phosphate dephosphorylation from PI(3,4,5)$P_3$ among WT and K364 mutants using $PH_{PLC\delta}$-GFP as probe for PI(4,5)$P_2$.**

(*A*) Representative fluorescence traces of $PH_{PLC\delta}$-GFP from insulin-pretreated oocytes. Depolarizing step shown in top of traces was applied from a holding potential of -60 mV to 50 mV for 10 seconds. Magnification of traces at the beginning of depolarization is shown in the right panel. (*B*) *Top*: Peak amplitude of transient fluorescence increase (*left*) and time to reach the peak from the beginning of depolarization (*right*) in WT and K364 mutants. *Bottom*: Peak amplitude vs time to reach the peak for each mutant. Data are presented as mean ± standard error (SE). ** p<0.01, n.s.; statistically not significant, one way ANOVA followed by Dunnett's test.